Supporting Information

Choi et al. 10.1073/pnas.0914140107

SI Materials and Methods

Purification of Tf-PEG-Sac. Fig. S1 presents data that confirm the purity of mono-PEGylated transferrin (Tf-PEG-SAc). The hydrophobic interaction chromatography analysis spectrum underscores the purity of the mono-PEGylated Tf. The MALDI-TOF spectrum indicates the apparent molecular weight of mono-PEGylated Tf as 84 kDa.

Binding Affinity of Tf-PEG-Sac. Fig. S2*A* illustrates the expression of Tf receptors (TfRs) on Neuro2A cells. Fig. S2*B* is the Scatchard plot based on the saturation binding curve shown in Fig. 1*C*. The slope of a Scatchard plot gives the inverse of the binding dissociation constant, K_d^{-1}. Linear regression gives K_d^{-1} = 0.0157 nM^{-1}, and thus K_d (Tf conjugated to AlexaFluor488; Tf-AF488) = 64 nM. K_d (Tf) ~ K_d (Tf-AF488) = 64 nM.

Estimation of Tf Content. Table S1 presents estimates of Tf content of Tf-PEG-gold nanoparticles (AuNPs) from the reaction of various amounts of Tf- thiolated poly(ethylene glycol) (Tf-PEG-SH) and 2.25 × 10^{10} unmodified 50-nm AuNPs in a 0.5 -L aqueous solution.

Binding Affinity of Tf-PEG-AuNP. Because of the in vitro binding curves of Tf-PEG-AuNPs (Fig. 3*C*), a Scatchard analysis yields an effective K_d of 1.06 and 0.13 nM for IV and V, respectively (Fig. S4). The binding data for III do not warrant a meaningful estimation of a K_d because of the low signal-to-noise ratio. Based purely on the Scatchard analysis, the K_d illustrates the binding affinity of the particle assuming 100% contact of all Tfs mounted on the surface of PEG-AuNPs. Because of particle curvature, this assumption is not realistic. Is there an approximation that evaluates the actual fraction of Tf in contact with the cell surface?

Estimates of Nanoparticle Binding Affinities to Cell Surface. Consider a sphere of radius R whose center is of a distance h away from a flat surface. The spherical curvature dictates the appropriate length scaling (Fig. S3). The sphere represents a PEGylated gold nanoparticle (II), whereas the flat surface represents a cellular surface that has an overexpression of TfRs. The distance between the sphere and the flat surface reflects the approximate height of Tf. By the Pythagorean theorem, $(z-h)^2 + r^2 = R^2$ For the bottom of sphere, and performing a Taylor expansion about the origin assuming $r << R$, we derive the following mathematical relationship:

$$z = h - R\sqrt{1-\left(\frac{r}{R}\right)^2} \approx h - R\left[1 - \frac{1}{2}\left(\frac{r}{R}\right)^2 + O\left(\frac{r}{R}\right)^4\right], \frac{z}{\varepsilon R} \sim 1 + \frac{1}{2\varepsilon}\left(\frac{r}{R}\right)^2 + \ldots$$

In these expressions, $\varepsilon = \frac{h-R}{R} = \frac{d}{R}$ and d is the distance of the thin gap between the bottom of sphere and the flat surface. If $r \sim R$, $z/\varepsilon R$ is huge and does not converge because $1/\varepsilon$ is huge. If $r << R$, $z/\varepsilon R$ is small, and the second term of the expansion vanishes. To account for the curvature of the sphere, the second term of the expansion must be set to the same size as the first term (i.e., order 1). Then we have the relevant length scale in the radial direction that indicates contact of the sphere with the flat surface: $r \approx 2R\varepsilon^{1/2} = 2\sqrt{dR}$.

Hence the required fraction of contact is $\frac{\pi(2\sqrt{dR})^2}{4\pi R^2} = \frac{d}{R}$, with the assumption of homogeneous Tf distribution on the entire spherical surface of PEG-AuNPs ($4\pi R^2$). From Table 1, the hydrodynamic size of II in 1× PBS is 75 nm. Tf has a Stokes–Einstein diameter of 8 nm (1). These two measurements, R = 37.5 nm and d = 8 nm, together suggest that ~21.3% of the Tf attached to Tf-PEG-AuNP is in contact with cellular TfRs (d/R = 0.2 <1).

Table S2 displays the effective K_ds with and without the geometric assumption. From Fig. 1 *C* and *D*, the K_d of a single Tf-PEG-SAc ligand is 144 nM. Given the geometric assumption, the enhancement in binding affinity caused by multivalency is thus up to ~600-fold and ~4800-fold for IV and V, respectively.

1. Sato K, et al. (1997) Saccharated ferric oxide (SFO)-induced osteomalacia: In vitro inhibition by SFO of bone formation and 1,25-dihydroxy-vitamin D production in renal tubules. *Bone* 21:57–64.

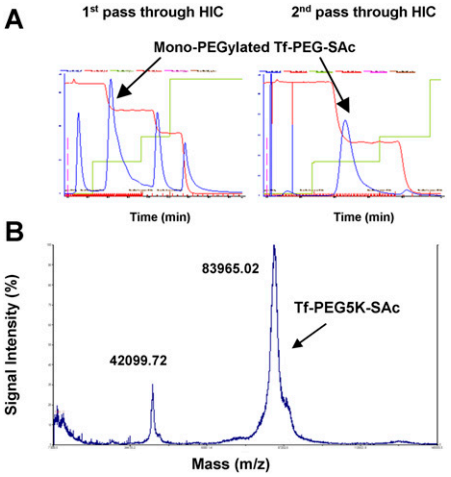

Fig. S1. Purification of Tf-PEG5K-SAc. (*A*) Hydrophobic interaction chromatography effectively purified the crude reaction mixture and separated out the mono-PEGylated fraction. (*B*) MALDI-TOF spectrum. The sharp peak at 84 kDa confirms the identity of the expected product, Tf-PEG-SAc.

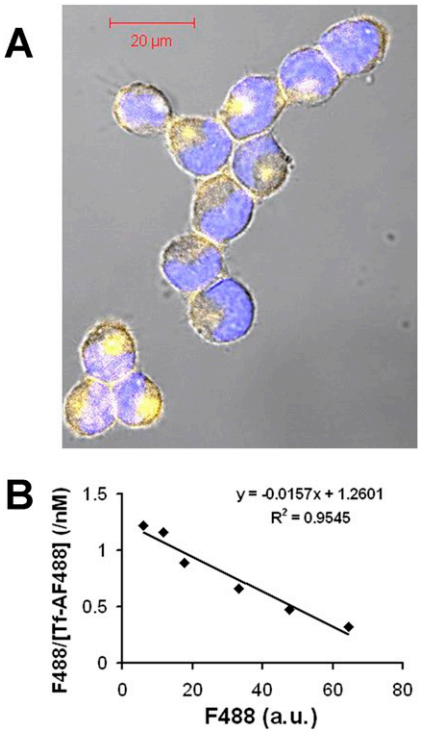

Fig. S2. Binding of Tf-AF488 on TfRs. (*A*) A confocal micrograph shows the surface and internalized TfRs of Neuro2A cells stained by antiTfR-AF555 (yellow), counterstained by DAPI nuclear stain (blue) (Scale bar, 20 μm.) (*B*) A Scatchard plot based on data from Fig. 1*C* yields an approximate K_d of 64 nM for Tf-AF488.

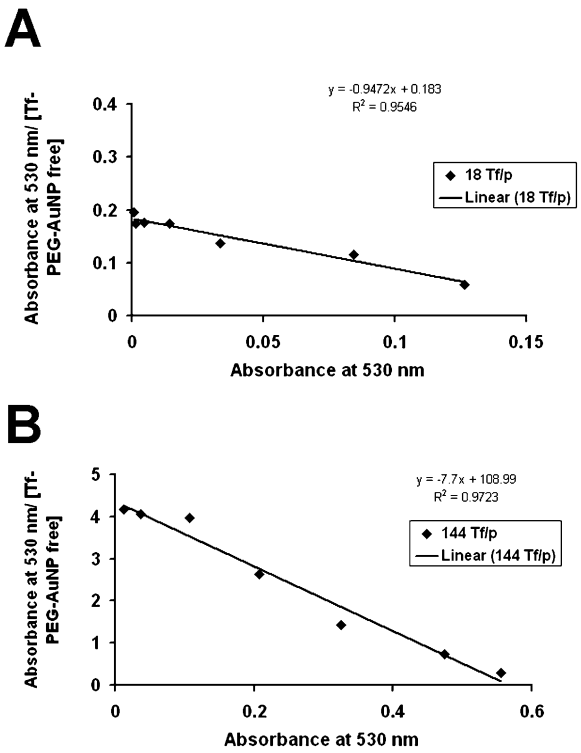

Fig. S3. Scatchard plots based on Fig. 3*C* yield a K_d of 1.06 and 0.13 nM for IV (*A*) and V (*B*), respectively.

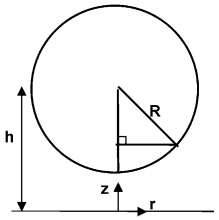

Fig. S4. Definition sketch of a sphere of radius R levitating on top of a flat surface.

Table S1. Coupling efficiency of Tf-PEG-AuNPs

	Mass of Tf-PEG-SH(ng)	Theoretical content(#Tf/particle)	Final content(#Tf/particle)	Coupling efficiency(%)
III	7.5	2.4	2.1 ± 0.2	86.6 ± 8.3
IV	75	24.2	17.5 ± 2.5	72.3 ± 10.3
V	750	241.8	144.3 ± 15.6	59.7 ± 6.5

The theoretical content assumes perfect conjugation of Tf-PEG-SH added to the reaction mixture. An ELISA was used to determine the amount of free Tf-PEG-SH, which in turn was used to deduce the amount of Tf-PEG-SH bound onto AuNPs (by assuming a perfect mass balance). A division of the final content by the theoretical content and multiplication by 100% gives the coupling efficiency.

Table S2. Multivalency of Tf-PEG-AuNPs

	K_d (nM) perfect contact	K_d (nM)21.33% contact	Binding enhancement
IV (18 Tf/particle)	1.06	0.23	~600-fold
V (144T f/particle)	0.13	0.03	~4800-fold

This enhancement in binding affinity (as seen from the effective Kds) by three orders of magnitude for IV and V highlights the effect of multivalency.